

Negative spin Hall magnetoresistance in antiferromagnetic Cr₂O₃/Ta bilayer at low temperature region

Yang Ji¹, J. Miao,^{1,a)} Y. M. Zhu¹, K. K. Meng,¹ X. G. Xu,¹ J. K. Chen¹, Y. Wu,¹ and Y.
Jiang^{1,b)}

*School of Materials Science and Engineering, University of Science and Technology
Beijing, Beijing, 100083, China*

ABSTRACT

We investigate the observation of negative spin Hall magnetoresistance (SMR) in antiferromagnetic Cr₂O₃/Ta bilayers at low temperature. The sign of the SMR signals is changed from positive to negative monotonously from 300 K to 50 K. The change of the signs for SMR is related with the competitions between the surface ferromagnetism and bulky antiferromagnetic of Cr₂O₃. The surface magnetizations of α -Cr₂O₃ (0001) is considered to be dominated at higher temperature, while the bulky antiferromagnetics gets to be robust with decreasing of temperature. The slopes of the abnormal Hall curves coincide with the signs of SMR, confirming variational interface magnetism of Cr₂O₃ at different temperature. From the observed SMR ratio under 3 T, the spin mixing conductance at Cr₂O₃/Ta interface is estimated to be $1.12 \times 10^{14} \Omega^{-1} \cdot \text{m}^{-2}$, which is comparable to that of YIG/Pt structures and our early results of Cr₂O₃/W. (Appl. Phys. Lett. 110, 262401 (2017))

^{a)} Electronic mail: j.miao@ustb.edu.cn

^{b)} Electronic mail: yjiang@ustb.edu.cn

Keywords:

Negative spin Hall magnetoresistance; $\text{Cr}_2\text{O}_3/\text{Ta}$ structure; Surface ferromagnetisms;

Bulky antiferromagnetisms;

The resistance of ferromagnetic materials (FMs) change depending on the magnitude of the external magnetic field, which is called magnetoresistance (MR). So far giant magnetoresistance (GMR),^[1,2] anisotropic magnetoresistance (AMR)^[3] and tunnel magnetoresistance (TMR)^[4-7] etc. have been discovered in the recent decades, but those MRs need a condition that the current must travel through the FMs, so these phenomenons only exist in conductive FMs. Moreover, spin Hall magnetoresistance (SMR) is a special MR that there is no charge current in the FM layer, which depends on the relative orientation between the magnetic moments of FM layer and the spin direction injected from normal metal (NM).^[8] H. Nakayama *et al.* first observed 0.01% MR ratio in YIG/Pt structure, and defined as SMR.^[9] Until now, SMR has been reported for NM/ferromagnetic insulators such as YIG,^[9-12] Fe₃O₄,^[13] NiFe₂O₄,^[14] and CoFe₂O₄^[15], etc..

It is known that the spin current plays an important role in the dynamics of SMR injecting from NM layer into magnetic layer. Due to the spin Hall effect (SHE), when the charge current flow through the NM layer, a spin current is generated in the vertical direction and pass the interface to arrive in FM layer. Meanwhile, the orientation relationship between the direction of the magnetic moment (**m**) in the magnetic layer and the polarization direction (**s**) of the spin current injected will determine the magnitude of the charge current by the inverse spin Hall effect (ISHE), which shows different resistance of NM layer, and lead to SMR.^[8,9]

In recent years, antiferromagnetic spintronics attract much research attentions.^[16,17] Han *et al.* detected SMR signal in the antiferromagnetic insulator SrMnO₃.^[18] Similarly, SMR has also been reported in antiferromagnetic metallic FeMn/Pt.^[19] A. Manchon investigated physical origin of SMR in the antiferromagnets and predicted that SMR can

be observable in other antiferromagnetic insulators such as NiO, CoO, Cr₂O₃ etc.^[20] In previous work, we observed a nearly 0.1% SMR ratio in Cr₂O₃/W with 9 T.^[21] Soon after that, a negative SMR has also been observed in NiO bulk crystal and films.^[22-24]

As known, Cr₂O₃ is insulating magnetoelectric antiferromagnet, in which the magnetism can be controlled by electric field.^[25] Due to its Néel temperature is 308 K, namely above the room temperature, which makes Cr₂O₃ become potential candidate material in antiferromagnetic spintronics. Recently T. Kosub put forth an concept of antiferromagnetic magnetoelectric random access memory, in which the prototypical memory cell consists of an active layer of Cr₂O₃.^[27] Relying on its advantages, more spintronic phenomenon will occur in Cr₂O₃ magnetoelectric. However, the physical mechanism in Cr₂O₃/heavy-metal structure has not been investigated in details.

In this work, we investigated the temperature dependence of SMR in a Cr₂O₃ (25)/Ta (5) bilayer, and confirmed that negative SMR is originated from the magnetizations of Cr₂O₃. The (0001)-oriented Cr₂O₃ films were grown on the (0001) oriented rutile Al₂O₃ substrates via pulse laser deposition (PLD) with a base pressure of 5×10^{-8} mbar. Prior to the Cr₂O₃ growth, the substrate temperature was increased to 450 °C with a rate of 10 °C/min, and the thin film deposition was performed with an oxygen partial pressure of 0.05 mbar. Then the Cr₂O₃ film was deposited with a laser power of 1.8 J/cm² and a frequency of 3.0 Hz and the target to substrate distance was maintained at 5 cm during the deposition. The cooling process was carried under 10⁻⁶ oxygen partial pressure with a rate of 10 °C/min to room temperature. After deposition, a 5 nm film Ta was grown *in situ* on the Cr₂O₃ by magnetron sputtering, where the base pressure of the chamber was less than 8×10^{-8} mbar.

Finally, a hall bar for electrical measurements was fabricated by electron beam lithography and Ar ion etching.

The optical image and experimental hall geometry of Cr₂O₃/Ta bilayers are shown in Fig. 1(a). The size of Hall-bar is 400 μm×40 μm and a constant channel current **I** of 20 μA along the **x** direction, in which the Hall-bar structure was patterned onto the substrate. The phase structure of the Cr₂O₃ films was determined by X-ray diffraction using M21XVHF22 X-ray diffractometer with Cu/Kα. Fig. 1(b) shows the XRD ω-2θ scan for the Al₂O₃ (0001)/Cr₂O₃ (25 nm) sample. Obviously Cr₂O₃ (0006) and Cr₂O₃ (00012) peaks can be observed next to the substrate peak at 39.8° and 86.1°, respectively, which demonstrates uniaxial orientation growth of α-Cr₂O₃.^[25] In addition, the surface morphologies was checked by using a scanning probe microscopy in Fig. 1(c) and the root-mean-square roughness is 0.217 nm for 25 nm Cr₂O₃ film. The surface of Cr₂O₃ layer is relatively smooth without any cracks or pinholes, which is beneficial to growing the upper heavy metal Ta layer.

According to the SMR theory,^[8,9] a charge current flowing along the x direction in Ta layer generates a y-polarized spin current, flowing along the z direction and injecting into Cr₂O₃ layer. Depending on the orientation of moments of Cr₂O₃ with respect to the spin direction of spin current, the reflected spin current varies in the magnitude, which yields an additional charge current via ISHE superimposed on the original charge current. as known, the SMR is described as^[8]

$$\rho_{xx} = \rho_0 - \Delta\rho m_y^2, \quad , \quad (1)$$

$$\frac{\Delta\rho_1}{\rho} = \theta_{SH}^2 \frac{\lambda}{d_N} \frac{2\lambda G_r \tanh^2 \frac{d_N}{2\lambda}}{\sigma + 2\lambda G_r \coth \frac{d_N}{\lambda}}, \quad , \quad (2)$$

where ρ_0 is a constant resistivity offset, \mathbf{m}_y is the y component of the magnetization unit vector, and $\Delta\rho_1/\rho$ depends on spin diffusion length λ , Ta layer thickness d_N , Ta electrical conductivity σ , spin hall angle θ_{SH} , and the real part of the spin mixing conductance G_r , as shown in Eq. (2).

Clearly, the in-plane field sweep cannot distinguish AMR from SMR since both signals depend on the orientation of moments in the **xy** plane. In order to extract the SMR contribution from the overall MR, both the field-dependent magnetoresistance (FDMR) measurements and angle-dependent magnetoresistance (ADMR) measurements were performed on the Cr₂O₃/Ta bilayer. As illustrated in Fig. 2(a), the longitudinal resistance of the sample was measured under rotating a constant field $H = 3$ T with α , β , γ , respectively. The different ADMR would reveals different physical mechanisms in two cases. i) if magnetic moments are rotated in the xz plane followed by angle γ , SMR should remain constant, since \mathbf{m}_y and the reflected spin current are unchanged, namely any resistance change can be attributed to AMR. ii) if moments are rotated in the yz plane followed by angle β , AMR should remain constant, since the charge current is always perpendicular to the moments, namely any resistance change can be attributed to SMR. However, if moments are rotated in the **xy** plane followed by angle α , both SMR and AMR change simultaneously and therefore the two MR effects are entangled.

Fig. 2(b) shows FDMR measurement at 300 K. Clearly, we can observe the MR in x-axis is the highest, and the MR in y-axis is the smallest. It should be noted that the magnetization of the bilayers is difficult to saturate, even the field is increased to 3 T. Fig. 2(c) shows the ADMR measurement with 3 T at 300 K, in which MR dependence on β -angle represents SMR and MR dependence on γ -angle represents AMR, respectively. A

conventional positive SMR can be observed and the SMR ratio is $(R_z - R_y)/R_z = 2.4 \times 10^{-4}$. Similarly, FDMR and ADMR measurements at 50 K are exhibited in Fig. 2(d) and Fig. 2(e). Interestingly, Comparing with MRs at 300 K, both FDMRs and ADMRs reverse their signs at 50 K, in which a negative SMR can be observed clearly. The ratio of SMR in $\text{Cr}_2\text{O}_3/\text{Ta}$ bilayer is about 0.5×10^{-4} , which is close to that of NiO/Pt structure.^[24]

To confirm those observations, Fig. 3(a) shows the longitudinal resistance R_{xx} dependence on β -angle for $\text{Cr}_2\text{O}_3/\text{Ta}$ bilayer with 3 T at different temperature. The corresponding temperature dependence of SMR were described in Fig. 3(b). Unambiguously, as temperature decreasing, SMR varies from positive to negative monotonically. When the sample was cooled down to 250 K, the positive SMR would decrease to zero sharply. As the temperature decreased further, the negative SMR gradually emerged. Nevertheless, the slope of the SMR curve starts to slow down below 250 K, and the ratio of SMR reaches a stable value until 50 K.

To investigate its physical origination, the magnetization structure of Cr_2O_3 need to be taken into account. As known, a boundary magnetization exists at the surface of the magnetoelectric antiferromagnet (0001) Cr_2O_3 .^[25,26] Therefore, as shown in Fig. 4(a), the magnetisms of Cr_2O_3 can be discriminated into two parts: surface ferromagnetism and bulk antiferromagnetism. Both of two parts will make contributions to SMR of $\text{Cr}_2\text{O}_3/\text{Ta}$. When the temperature is higher than 250 K, the antiferromagnetic order in Cr_2O_3 is weaker and its corresponding contribution to SMR is less than that from surface ferromagnetism. Thus, the sign of SMR shows positive, like FM/NM structure such as YIG/Pt .^[9-12] Oppositely, when the temperature is below 250 K, the antiferromagnetic order gets strong and surface ferromagnetism gets weaker. Thus, the contributions from antiferromagnetic order is more

than that contributed from surface ferromagnetism to SMR. Therefore, the sign of SMR in Cr₂O₃/Ta shows negative. A similar phenomenon has been reported in NiO/Pt structure.

[22-24]

It should be noted that only the β -phase of Ta has a large spin Hall angle and strong spin-orbit coupling than other phase of Ta, so ρ_{xx} as a function of temperature for a 5-nm-thick Ta/Cr₂O₃ film sample was measured. As shown in Fig. 4(b), the high resistivity of β -phase Ta is agreed with that reported increases with decreasing temperature. [28,29] Furthermore, from the equation (2), a higher SMR ratio with help of β -Ta can be obtained. At the same time, the spin mixing conductance G_r can be estimated via the SMR ratio $\Delta\rho_1/\rho = 0.04\%$ with 3 T at 300 K. For Ta, [10] $\theta_{SH} = 0.02$, $\lambda = 1.8$ nm, $d_N = 5$ nm, and consequently the spin mixing conductance $G_r = 1.12 \times 10^{14} \Omega^{-1} \cdot m^{-2}$. Due to the MRs are unsaturated till 3 T, the values of G_r should be larger with increasing the magnetic field.

To confirm that explanations, the Hall resistance measurements were carried out in Cr₂O₃/Ta bilayer at different temperature, which are shown in Figs. 5(a) and 5(b). It should be noted that the transition temperature of Cr₂O₃ film is 250 K. i) when the temperature is higher than 250 K, the slopes of Hall curves are all positive and the abnormal Hall effect (AHE) can be observed. In addition, AHE signals of Cr₂O₃/Ta bilayer get stronger with increasing temperature, which is attributed to the surface ferromagnetism of Cr₂O₃. ii) when the temperature is lower than the transition temperature, the slopes of Hall curves are negative and no AHE signals can be observed. In other words, surface ferromagnetism may vanish with temperature decreasing, namely the bulk antiferromagnetic may exceed the surface ferromagnetism in the Cr₂O₃ thin films. [25]

In conclusion, we observed a negative SMR in $\text{Cr}_2\text{O}_3/\text{Ta}$ bilayers below 250 K, which is attributed to the competitions between the surface ferromagnetism and bulky antiferromagnetics of Cr_2O_3 . Above the transition temperature, the surface ferromagnetism of Cr_2O_3 is dominated, leading to a normal positive SMR. While the temperature is below the transition temperature, antiferromagnetic Néel order of Cr_2O_3 is robust and surface ferromagnetism makes less contributions to SMR, resulting in a negative SMR. The observations of negative SMR in antiferromagnet, like Cr_2O_3 , NiO , may pave a way for applications in antiferromagnetic spintronics devices.

ACKNOWLEDGEMENTS

This work was partially supported by the National Basic Research Program of China (Grant No. 2015CB921502), the National Science Foundation of China (Grant Nos. 11574027, 51731003, 51671019, 51471029) and Beijing Municipal Science and Technology Program (Z161100002116013) and Beijing Municipal Innovation Environment and Platform Construction Project (Z161100005016095). J.C., K.M., and Y.W. acknowledge the National Science Foundation of China (Nos. 61674013, 51602022, 61404125, 51501007).

REFERENCES

1. M. N. Baibich, J. M. Broto, A. Fert, F. Nguyen Van Dau, and F. Petroff, Phys. Rev. Lett. **61**, 2472 (1988).
2. G. Binasch, P. Griinberg, F. Saurenbach, and W. Zinn, Phys. Rev. B **39**, 4828 (1989).
3. T. R. Mcguire and R. I. Potter, IEEE Trans. Magn. **11**, 1018 (1975).
4. J. S. Moodera, L. R. Kinder, T. M. Wong, and R. Meservey, Phys. Rev. Lett. **74**, 3273 (1995).
5. T. Miyazaki and N. Tezuka, J. Magn. Magn. Mater. **139**, L231 (1995).
6. S. S. P. Parkin, C. Kaiser, A. Panchula, P. M. Rice, B. Hughes, M. Samant, and S. H. Yang, Nat. Mater. **3**, 862 (2004).
7. S. Yuasa, A. Fukushima, T. Nagahama, K. Ando, and Y. Suzuki, Nat. Mater. **3**, 868 (2004).
8. Y.-T. Chen, S. Takahashi, H. Nakayama, M. Althammer, S. T. B. Goennenwein, E. Saitoh, and G. E. W. Bauer, Phys. Rev. B **87**, 144411 (2013).
9. H. Nakayama, M. Althammer, Y.-T. Chen, K. Uchida, Y. Kajiwara, D. Kikuchi, T. Ohtani, S. Geprägs, M. Opel, S. Takahashi, R. Gross, G. E. W. Bauer, S. T. B. Goennenwein, and E. Saitoh, Phys. Rev. Lett. **110**, 206601 (2013).
10. C. Hahn, G. de Loubens, O. Klein, and M. Viret, Phys. Rev. B **87**, 174417 (2013).
11. N. Vlietstra, J. Shan, V. Castel, and B. J. van Wees, Phys. Rev. B **87**, 184421 (2013).
12. N. Vlietstra, J. Shan, V. Castel, J. Ben Youssef, G. E. W. Bauer, and B. J. van Wees, Appl. Phys. Lett. **103**, 032401 (2013).
13. Z. Ding, B. L. Chen, J. H. Liang, J. Zhu, J. X. Li, and Y. Z. Wu, Phys. Rev. B **90**, 134424 (2014).
14. M. Althammer, S. Meyer, H. Nakayama, M. Schreier, S. Altmannshofer, M. Weiler, H. Huebl, S. Geprägs, M. Opel, R. Gross, D. Meier, C. Klewe, T. Kuschel, J. Schmalhorst, G. Reiss, L.

- Shen, A. Gupta, Y.-T. Chen, G. E. W. Bauer, E. Saitoh, and S. T. B. Goennenwein, *Phys. Rev. B* **87**, 224401 (2013).
15. M. Isasa, A. Bedoya-Pinto, S. Vélez, F. Golmar, F. Sánchez, L. E. Hueso, J. Fontcuberta, and F. Casanova, *Appl. Phys. Lett.* **105**, 142402 (2014).
 16. E. V. Gomonay, and V. M. Loktev, *Low Temp. Phys.* **40**, 17 (2014).
 17. T. Jungwirth, X. Marti, P. Wadley, and J. Wunderlich, *Nat. Nanotechnol.* **11**, 231 (2016).
 18. J. H. Han, C. Song, F. Li, Y. Y. Wang, G. Y. Wang, Q. H. Yang, and F. Pan, *Phys. Rev. B* **90**, 144431 (2014).
 19. Y. Yang, Y. Xu, K. Yao, and Y. Wu, *AIP Adv.* **6**, 65203 (2016).
 20. A. Manchon, *Phys. Status Solidi RRL* **11**, 1600409 (2017).
 21. Y. Ji, J. Miao, K. K. Meng, Z. Y. Ren, B. W. Dong, X. G. Xu, Y. Wu, and Y. Jiang, *Appl. Phys. Lett.* **110**, 262401 (2017).
 22. G. R. Hoogeboom, A. Aqeel, T. Kuschel, T. T. M. Palstra, and B. J. van Wees, *Appl. Phys. Lett.* **111**, 52409 (2017).
 23. J. Fischer, O. Gomonay, R. Schlitz, K. Ganzhorn, N. Vlietstra, M. Althammer, H. Huebl, M. Opel, R. Gross, S. T. B. Goennenwein, and S. Geprägs, preprint arXiv: 1709.04158 (2017).
 24. L. Baldrati, A. Rossi, T. Niizeki, C. Schneider, R. Ramos, J. Cramer, O. Gomonay, M. Filianina, T. Savchenko, D. Heinze, A. Kleibert, E. Saitoh, J. Sinova, and M. Kläui, preprint arXiv: 1709.00910 (2017).
 25. X. He, Y. Wang, N. Wu, A. N. Caruso, E. Vescovo, K. D. Belashchenko, P. A. Dowben, and Ch. Binek, *Nat. Mater.* **9**, 579 (2010).
 26. L. Fallarino, A. Berger, and Ch. Binek, *Appl. Phys. Lett.* **104**, 022403 (2014).

- 27. T. Kosub, M. Kopte, R. Hühne, P. Appel, B. Shields, P. Maltinsky, R. Hübner, M. O. Liedke, J. Fassbender, O. G. Schmidt, and D. Makarov, Nat. Commun. **8**, 13985 (2017).
- 28. L. Q. Liu, C.-F. Pai, Y. Li, H. W. Tseng, D. C. Ralph, and R. A. Buhrman, Science **336**, 555 (2012).
- 29. M. Morota, Y. Niimi, K. Ohnishi, D. H. Wei, T. Tanaka, H. Kontani, T. Kimura, and Y. Otani, Phys. Rev. B **83**, 174405 (2011).

FIGURE LEGENDS

Fig. 1 (a) Optical image of the $\text{Cr}_2\text{O}_3/\text{Ta}$ bilayer surface and a schematic illustration of the electric resistance measured by the four-probe method, in which the length is 400 μm , and the width is 40 μm . (b) XRD 2θ scan from the 25 nm Cr_2O_3 film grown on Al_2O_3 (0001) substrate. (c) of 25 nm Cr_2O_3 film and the R_q is 0.217 nm.

Fig. 2 (a) Notations of different rotations of the angular α , β , and γ . (b) and (d) show external magnetic field dependence of resistance curve for Cr_2O_3 (25)/Ta (5) at 300 K (b) and at 50 K (d). (c) and (e) show α , β , and γ dependence of resistance curve for Cr_2O_3 (25)/Ta (5) with 3 T magnetic field at 300 K (c) and at 50 K (e).

Fig. 3 (a) β dependence of the resistance in Cr_2O_3 (25)/Ta (5) with 3 T magnetic field at different temperature. (b) Temperature dependence of SMR signals in Cr_2O_3 (25)/Ta (5) under 3 T.

Fig. 4 (a) Schematic of Cr_2O_3 spin structure at $T < T_{\text{Néel}}$ in an AFM single domain state (lower two layers of arrows represent AFM structure of Cr^{3+} spins in the bulk), which is accompanied by a positive boundary magnetization (top layer representing the surface). (b) Resistivity as a function of temperature of a representative 5 nm thick Ta Hall bar/ Cr_2O_3 film by the four-probe method. Inset: the schematic illustration of measurement.

Fig. 5 AHE measurements of Cr_2O_3 (25)/Ta (5) at 50 -265 K (a) and 270 -300 K (b)

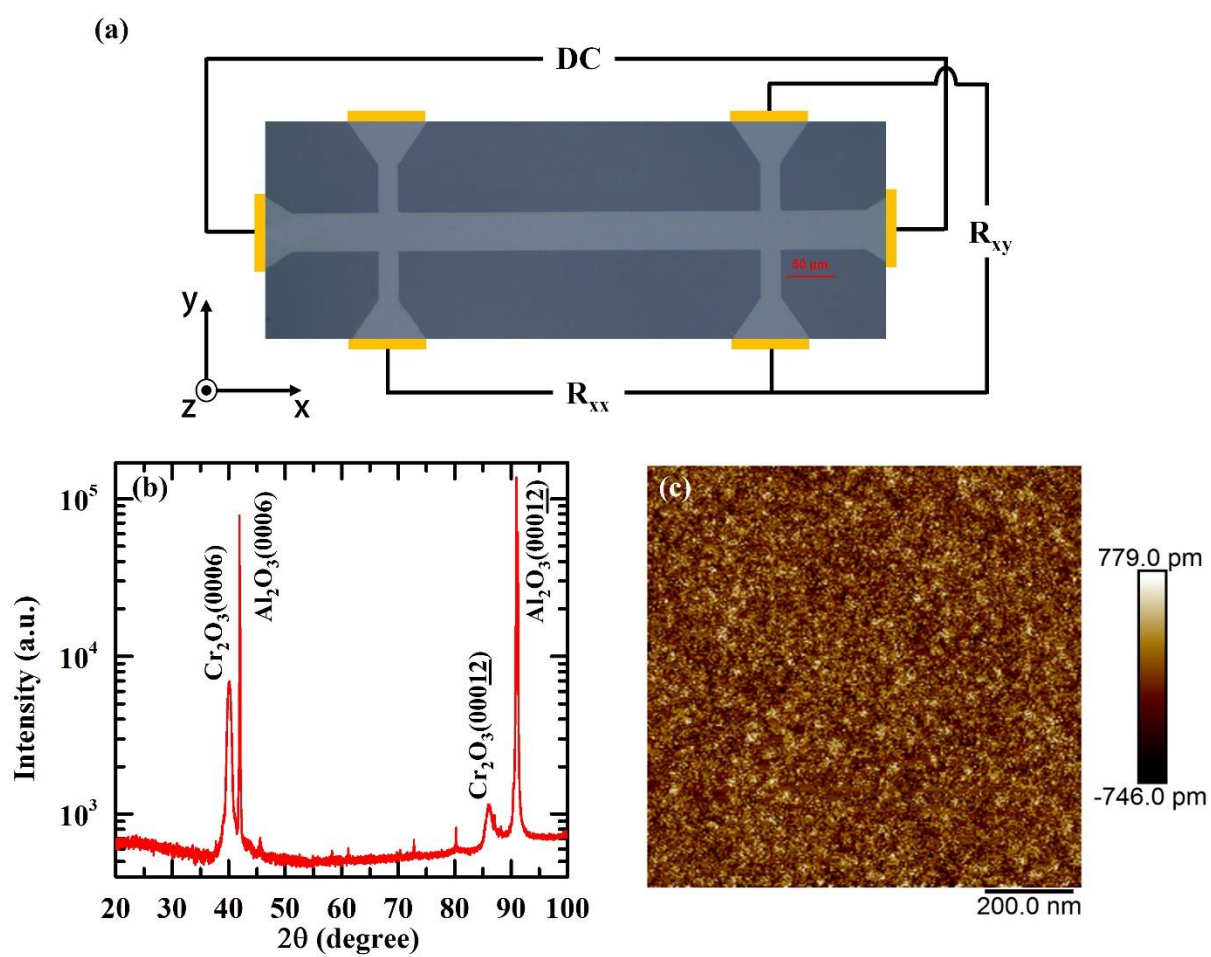


Fig. 1

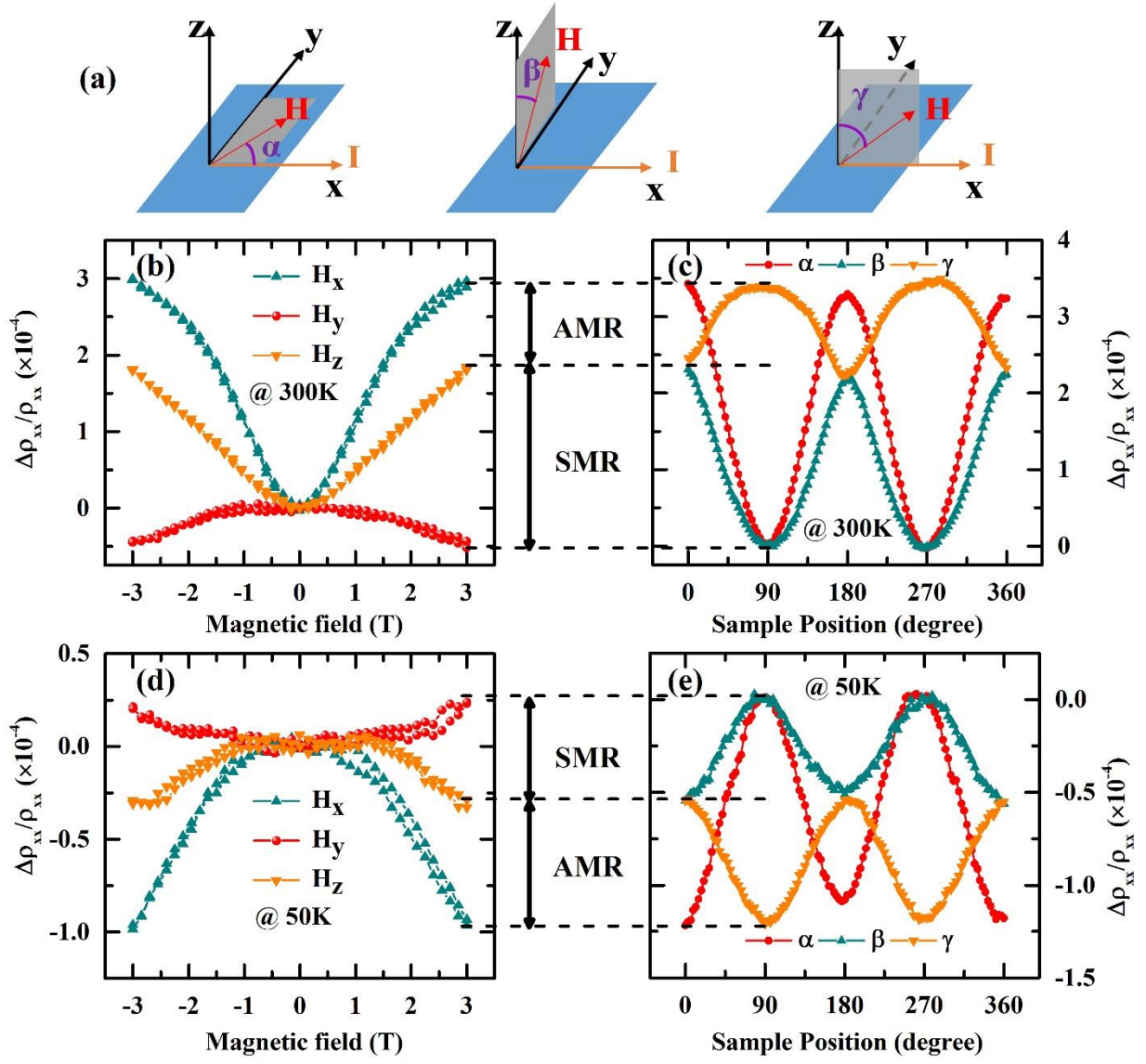


Fig. 2

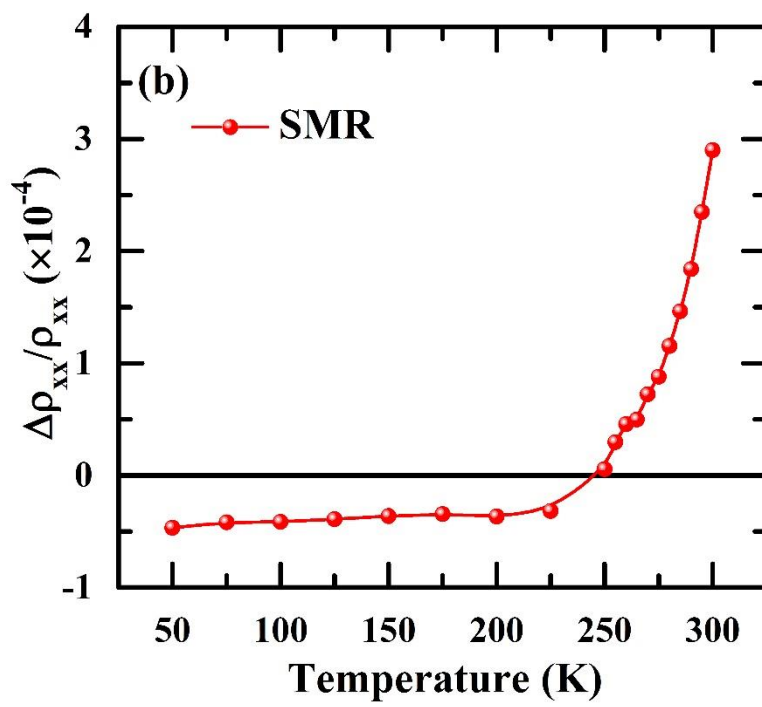
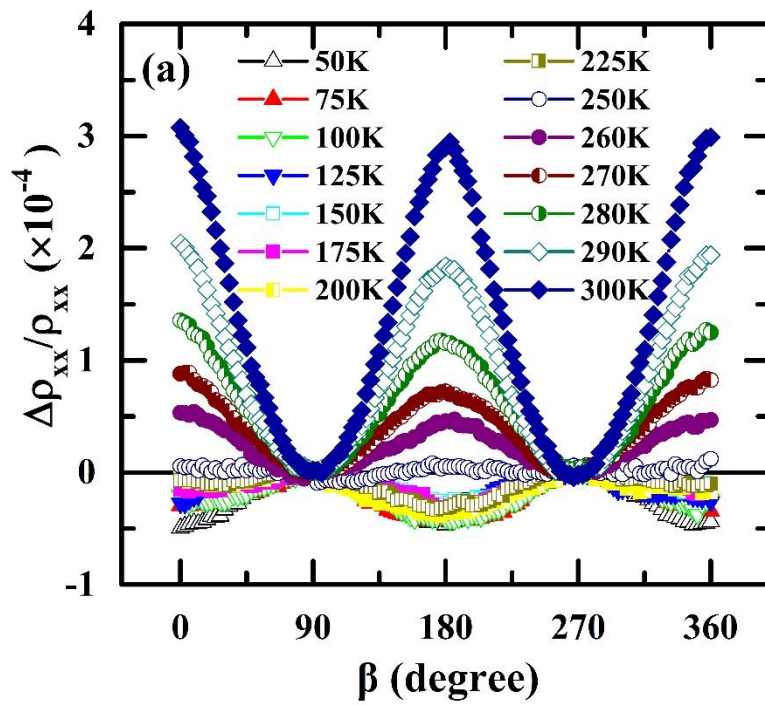


Fig. 3

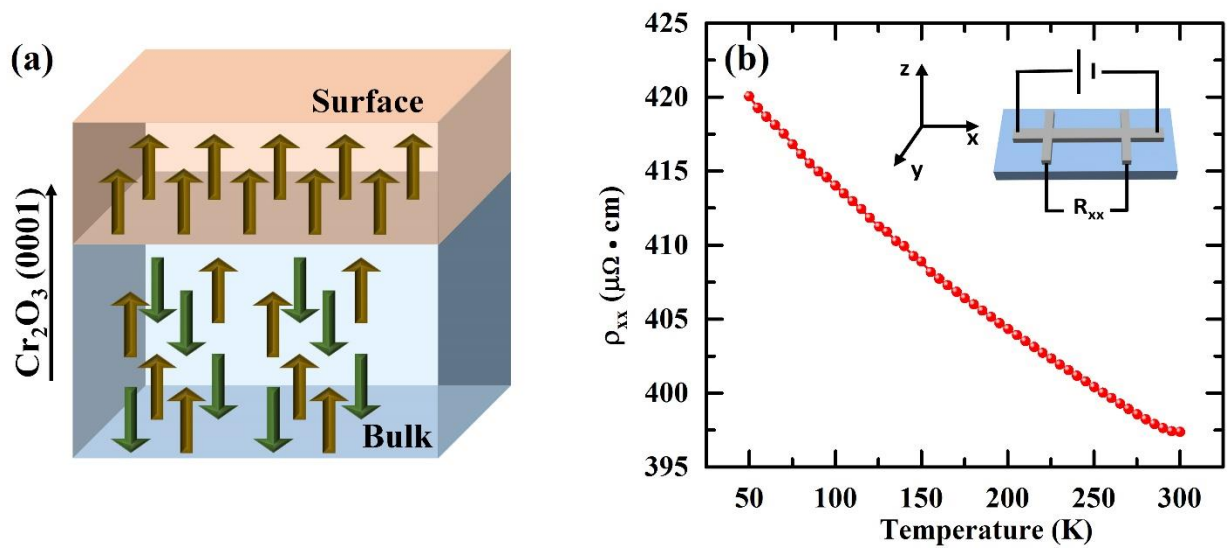


Fig. 4

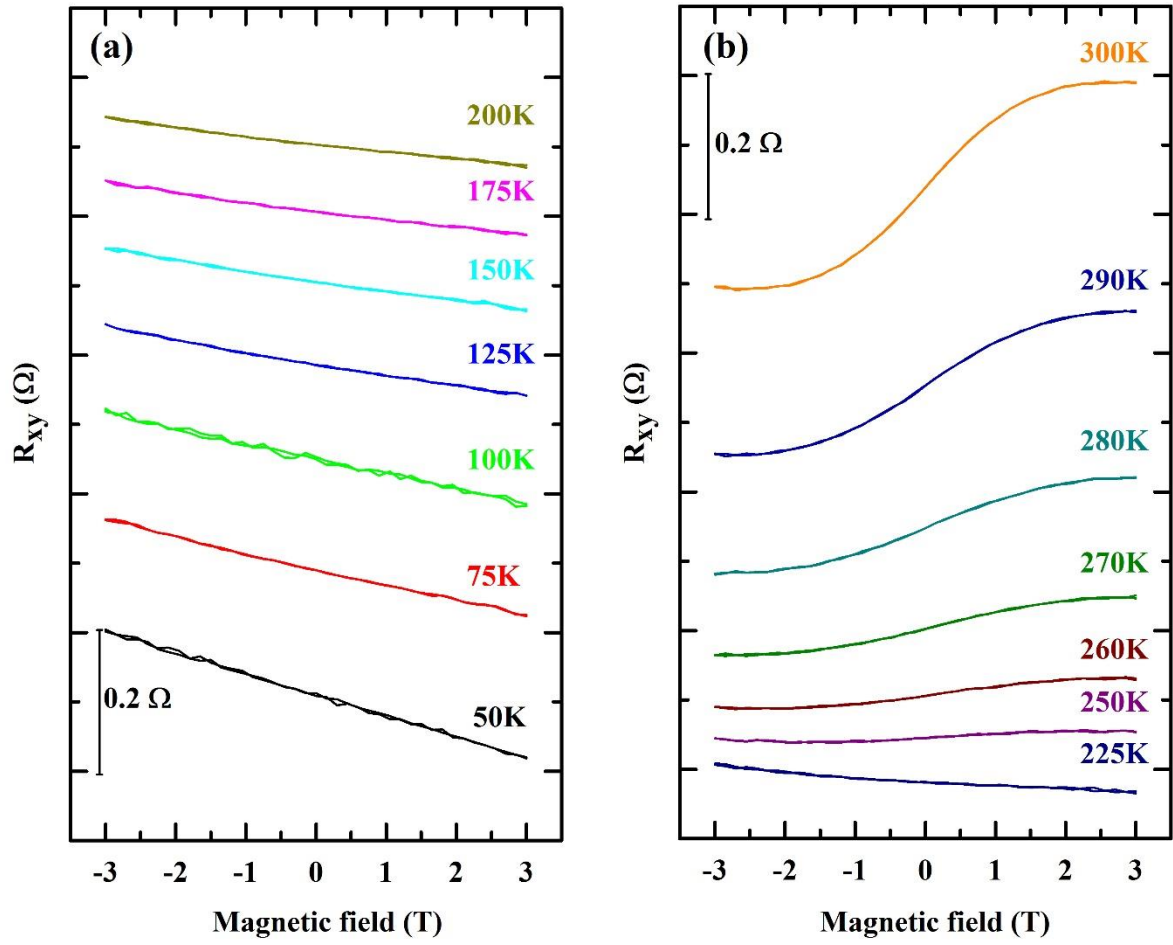


Fig. 5